Journal of the European Ceramic Society 23 (2003) 371–378

www.elsevier.com/locate/jeurceramsoc

Fabrication and characterisation of porous silicon nitride ceramics using Yb_2O_3 as sintering additive

Jian-Feng Yang[a,c,*], Zhen-Yan Deng[b], Tatsuki Ohji[c]

[a]*Japan Science and Technology Corporation (JST), Synergy Materials Research Center, AIST, Nagoya 463-8687, Japan*
[b]*Synergy Ceramics Laboratory, Fine Ceramics Research Association, Nagoya 463-8687, Japan*
[c]*National Institute of Advanced Industrial Science and Technology (AIST), Shidami Human Science Park, 2268-1, Simo-Shidami, Moriyama-ku, Nagoya 463-8687, Japan*

Received 28 December 2001; received in revised form 18 May 2002; accepted 1 June 2002

Abstract

Porous Si_3N_4 ceramics were fabricated by liquid-phase sintering with a Yb_2O_3 sintering additive, and the microstructure and mechanical properties of the ceramics were investigated, as a function of porosity. Low densification was achieved using a lower Yb_2O_3 additive content. Fibrous β-Si_3N_4 grains developed in the porous microstructure, and the grain morphology and size were affected by different sintering conditions. A high porosity, ~40–60%, with β-Si_3N_4 grain development, was obtained by adjusting the additive content. Superior mechanical properties, as well as strain tolerance, were obtained for porous ceramics with a microstructure of fine, fibrous grains of a bimodal size distribution.

Keywords: Mechanical properties; Porosity; Si_3N_4; Sintering

1. Introduction

Porous ceramic materials have many industrial applications as filtering materials, including uses as high-temperature gas filters, separation membranes, and catalyst supports. For such applications, a high porosity (typically >40%) of channels, with a well-controlled pore size distribution, is required. On the other hand, porous ceramic materials with a tailored microstructure are considered high-performance structural materials because of such unique properties as light weight, good strain tolerance, damage tolerance, and thermal shock resistance.[1–7] Some authors, for example, have reported that porous silicon nitrides with elongated fibrous β-Si_3N_4 grains that are one-directionally aligned show a high fracture energy, ~500 J/m^2, as well as a high strength, >1 GPa, and a low Young's modulus, ~240 GPa.[5,7]

Silicon nitride ceramics possess superior mechanical properties at both room temperature and high temperature. Thus, porous Si_3N_4 also has some potential for use as an engineering material, and some processes have been developed to produce the porous Si_3N_4 ceramics.[7–9] Sintering powder compacts to a fixed degree of densification, a process called *partial sintering*,[10,11] is generally used to fabricate porous ceramic materials composed of oxides. Because of the good sinterability of these materials, the density is adjusted by the heating characteristics, such as temperature and holding time. The sintering of Si_3N_4 ceramics is difficult, because of strong covalent bonding between silicon and nitrogen atoms, so that sintering additives are necessary for consolidating Si_3N_4 ceramics by liquid-phase sintering. On the other hand, the difficulty of sintering Si_3N_4 ceramics makes it possible to control densification (porosity) easily by adjusting the additives and the sintering process. By adjusting the characteristics of the sintering additive, such as the type and amount, porous Si_3N_4 ceramics can be obtained by the same sintering process used to obtain dense Si_3N_4 ceramics. Thus, a fibrous Si_3N_4 microstructure can be developed during

* Corresponding author at his second address. Tel.: +81-52-739-0156; fax: +81-52-739-0136.
E-mail address: jf-yang@aist.go.jp (J.-F. Yang).

0955-2219/02/$ - see front matter
PII: S0955-2219(02)00175-9

sintering, and excellent mechanical properties can be obtained,[6] compared with those of porous oxide ceramics obtained by partial sintering.

In the present study, we fabricated Si_3N_4 ceramics of various porosities using a Yb_2O_3 sintering additive and investigated the microstructures and mechanical properties of those ceramics, as a function of porosity. A usual liquid-phase sintering technique, with the usual powder compaction, was used to make the fabrication process simple and cost-effective.

The sintering additive, Yb_2O_3, is known to lead to crystalline $Yb_4Si_2O_7N_2$ formation at grain boundaries or triple junctions, even with no post heat treatment,[12,13] which presumably enhances the high-temperature mechanical properties of Si_3N_4 ceramics. The addition of Yb_2O_3 also is known to accelerate the fibrous grain growth of β-Si_3N_4,[14] a result that is advantageous for the strengthening effects of grain bridging and pullout. Furthermore, because of the high melting point of Yb_2O_3 and the high viscosity of Yb_2O_3-related glass, this additive is unsuitable for the densification of Si_3N_4, a characteristic that is, conversely, beneficial for the fabrication of porous Si_3N_4.

2. Experimental procedure

2.1. Materials

The raw materials used for the present study were commercial, high α-content Si_3N_4 powder (SN-E10, UBE Industries, Ltd., Tokyo, Japan; >95.5% α ratio, 1.3 wt.% oxygen, 0.55 μm particle size). Various contents (1–7.5 wt.%) of Yb_2O_3 (99.9% purity, High Purity Chemical Co., Tokyo, Japan) were used as a sintering additive. The mixture was wet-milled in methanol for 24 h, using high-purity Si_3N_4 grinding media. After the powder mixture had been dried using an evaporator, it was sieved to a particle size <500 μm. The resulting powder mixtures were uniaxially pressed, at 20 MPa, into rectangular bars measuring 64×6.5×5 mm. The relative densities of the green bodies were ~42–45% of theoretical density. The pressed green compacts were placed in a BN-coated graphite case and sintered in a graphite resistance furnace (Model No. FVPHP-R-5, Fujidempa Kogyo Co., Ltd., Osaka, Japan), at various temperatures between 1600 and 1850 °C, under a nitrogen-gas pressure of 0.6 MPa. The heating rate was 10–20 °C/min, and holding times were 2 h.

2.2. Microstructural characterization and mechanical test

The bulk density and porosity of the sintered samples were measured by the Archimedes displacement method, using distilled water. The theoretical density was calculated by the rule of mixtures. The samples were machined into 40–50×4×3 mm test bars for flexural-strength measurements, at room temperature, according to JIS R1601. All surfaces were finish-ground with an 800-grit diamond wheel. The tensile edges were beveled to reduce the effect of edge cracks. The samples were loaded to failure in a three-point bend fixture (with a span of 30 mm), on a testing machine (Model No. Autograph AG-10TC, Shimadzu Corp., Kyoto, Japan), at a cross-head speed of 0.5 mm/min. Young's modulus was measured by the pulse echo method. The strength and Young's modulus data were the average of six measurements. The failure strain was equal to the flexural strength divided by the Young's modulus.

Crystalline phases were identified by X-ray diffractometry (XRD; Model No. RINT 2000, Rigaku Co., Ltd., Tokyo, Japan), using CuK_α radiation at 40 kV and 100 mA. The pore size distribution of the porous ceramic was determined by mercury porosimetry (Autopore II 9220, Shimadzu Corp., Kyoto, Japan). The microstructure was characterized by scanning electron microscopy (SEM; Model No. S-5000, Hitachi Co., Ltd., Tokyo, Japan). The fracture surfaces of the bending test, coated with gold, were used for SEM observation. Grain width and length were measured for the individual grains from the SEM photos of the fracture surfaces. Due to the high porosity, the grain width was three-dimensionally visible. More than 500 grains were measured statistically for each sample, and relationship between grain area fraction and corresponding grain width were plotted to represent the grain distribution.

3. Results and discussion

3.1. Densification

Variations in the relative density with additive contents and sintering temperature are shown in Fig. 1.

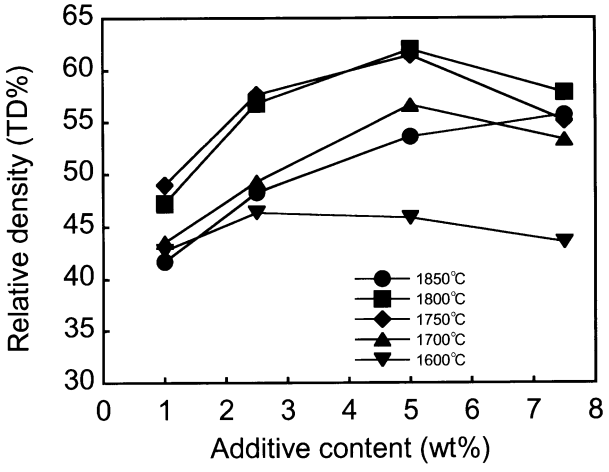

Fig. 1. Variations in density of porous Si_3N_4 ceramic as a function of additive contents and sintering temperature.

With an increase in additive contents, the density increased at first, but decreased at an additive content as high as 7.5 wt.%. At 1600 °C, the densities of the sintered samples were almost the same as that of the green body, indicating that no densification had occurred. Increasing the sintering temperature promoted densification. However, sintering at 1850 °C led to a substantial decrease in density. For all of the samples, the density was in the range 42–62% of the theoretical value. Increasing the sintering time had little effect on density.

Usually, the densification of Si_3N_4 with Y_2O_3–Al_2O_3 or Yb_2O_3–Al_2O_3 sintering additives starts at ~1400–1500 °C, and >90% relative density is achieved for a sample with a high additive content.[15,16] The additives react with SiO_2 on the surface of the Si_3N_4 grains to produce a glass or crystalline phase. When Yb_2O_3 alone is used as a sintering additive, a very thin boundary layer forms at the grain boundaries, and crystalline $Yb_4Si_2O_7N_2$ forms at the triple junctions. This crystalline phase has a high melting point; thus, densification is inhibited, compared to the situation with Y_2O_3–Al_2O_3 additives.

As a result, hardly any densification occurred at 1600 °C for the present samples with 1–7.5 wt.% Yb_2O_3, and increasing the sintering temperature did not result in complete densification. Compared with the nearly full densification of the samples with Y_2O_3–Al_2O_3 additives, a density as low as ~60% of the theoretical value was obtained with addition of Yb_2O_3, even for the sample sintered at 1800 °C.

Increasing the additive content also enhanced the densification, as expected, a result that could be mainly attributed to particle rearrangement. On the other hand, increasing the Yb_2O_3 content to 7.5 wt.% led to a decrease in density. Park et al. [14] indicated that coarse, elongated Si_3N_4 grains developed with 8 wt.% Yb_2O_3 addition. On the contrary, only fine Si_3N_4 grains existed with 4 wt.% Yb_2O_3 addition. Our previous research[15,16] revealed that phase transformation and grain growth delay densification, because of the impingement of the fibrous grains. In this present study, the development of β-Si_3N_4 grains is thought to be the main reason for the decrease in the density of the sample with 7.5 wt.% Yb_2O_3 addition, a theory discussed in the next section.

3.2. Phase transformation and microstructure

The microstructures of the resultant Si_3N_4 porous ceramics after sintering at different temperatures are shown in Fig. 2. The microstructure of the sample sintered at 1600 °C consisted of fine, equiaxed grains only. The average grain size was almost the same as that of the starting powder, indicating minimal phase transformation, which can also be confirmed by XRD analysis as only α-Si_3N_4 peaks were identified. Because the density after sintering exhibited little change, compared with that of the green compact, complete sintering was not achieved at this temperature. Increasing the sintering temperature caused the formation and development of β-Si_3N_4 grains, indicating enhanced phase transformation

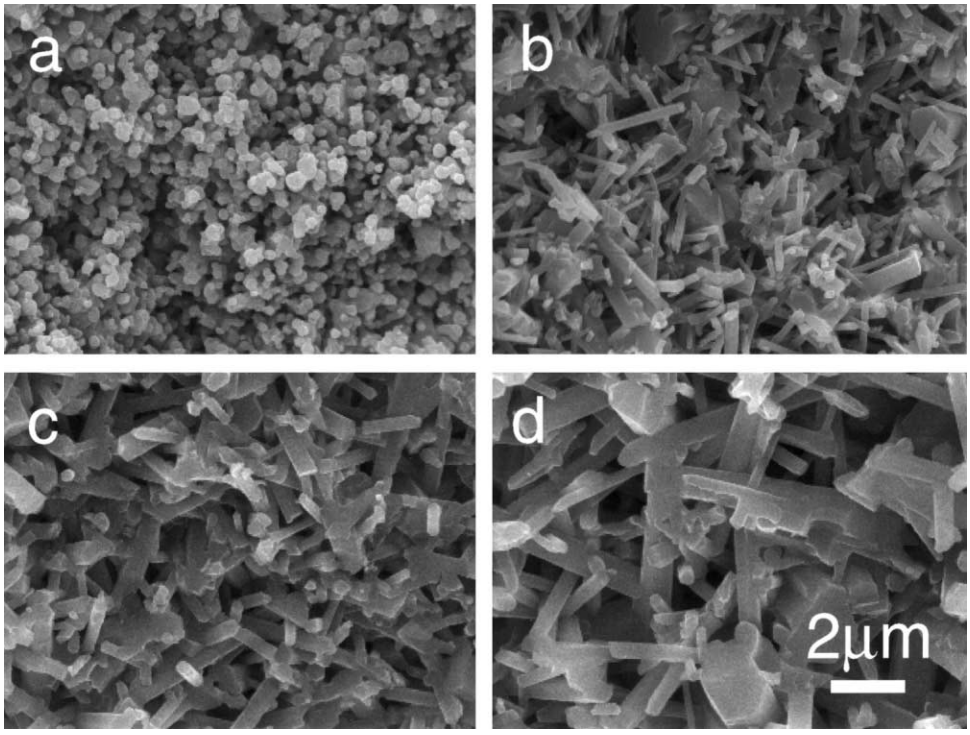

Fig. 2. SEM photographs of porous Si_3N_4 ceramic with 5 wt.% Yb_2O_3 sintered at (a) 1600 °C, (b) 1700 °C, (c) 1800 °C and (d) 1850 °C, respectively.

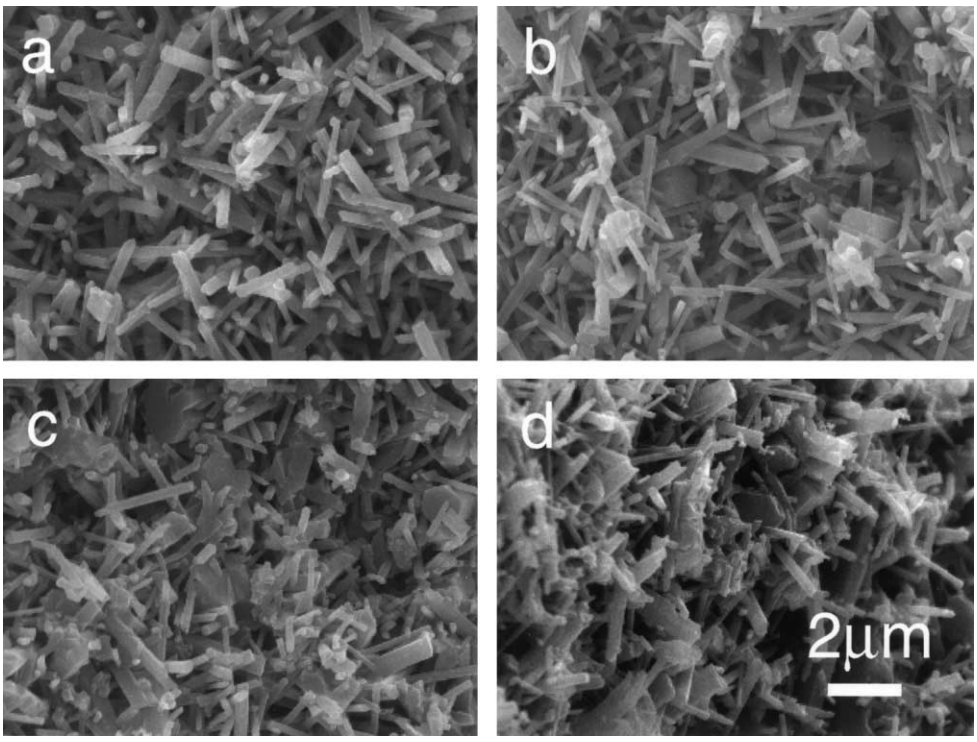

Fig. 3. SEM photographs of porous Si_3N_4 ceramic doped with (a) 1 wt.%, (b) 2.5 wt.%, (c) 5 wt.% and (d) 7.5 wt.% Yb_2O_3, respectively. The samples were sintered at 1700 °C.

and grain growth. When the sample was sintered at 1700 °C, very fine, fibrous β-Si_3N_4 grains were obtained, and medium-sized grains appeared at 1800 °C. When the sintering temperature was increased to 1850 °C, coarse grains dominated. As a side note, the aspect ratio of fibrous Si_3N_4 grains depends on the interfacial energy anisotropy between the longitudinal and the transverse surfaces.[17]

Fig. 3 shows the microstructures of samples with different contents of Yb_2O_3 additive, after sintering at 1700 °C for 2 h. The top 10 grains with largest width and their area was measured, and their average value and area fraction were shown in Table 1. The sample with 1 wt.% Yb_2O_3 consisted of fine Si_3N_4 grains only and low fraction of the largest grains. However, increasing the Yb_2O_3 content resulted in the formation of large, elongated Si_3N_4 grains in the fine matrix, as shown in Fig. 3(b)–(d) and Table 1. This phenomenon is consistent with the results of Park et al.[14] which showed that the microstructures of the samples with a Yb_2O_3 content >8 wt.% and those with <8 wt.% Yb_2O_3 were quite different. Large, elongated Si_3N_4 grains appeared when the Yb_2O_3 content was >8 wt.%, because of the large amounts of liquid phase. In the present study, super-large, elongated Si_3N_4 grains also formed, and their number increased with an increase in additive content, even when the samples were sintered at 1700 °C. The existence of the super-large grains in the Si_3N_4 ceramics is explained by the additive characteristics, such as the amount and nature of the liquid phase.[18]

Table 1
Average grain size and area fraction of top 10 largest grain of porous Si_3N_4 ceramic doped with various Yb_2O_3 content in Fig. 3. The samples were sintered at 1700 °C

Sample number	Yb_2O_3 content (wt.%)	Relative density (TD%)	Average width (μm)	Area fraction (%)
1	1.0	43.6	0.48	6.8
2	2.5	49.3	0.79	8.6
3	5.0	56.6	0.90	11.4
4	7.5	53.3	0.87	12.8

Compared to Y_2O_3, a lanthanide oxide shows a tendency to form high-aspect-ratio β-Si_3N_4. As shown in Fig. 1, the addition of 7.5 wt.% Yb_2O_3 always decreases the density, as compared with the sample with 5 wt.% Yb_2O_3. This decrease occurs because the formation of more large, elongated Si_3N_4 grains decreases the density, due to the impingement of fibrous grains. This impingement effect also causes decreased density as the sintering temperature increases.[15]

Relation between grain area and corresponding grain width was plotted in Fig. 4. It can be seen that sample sintered at 1850 °C have a coarse grain width. With decreasing in sintering temperature, grain width was prone to becoming fine. Another microstructural feature for the samples sintered at 1700 °C is that some large, elongated Si_3N_4 grains developed in the fine Si_3N_4

matrix with increasing additive content, as discussed in the previous section and shown in Fig. 4. This type of microstructure is referred to as in situ reinforcement in ceramics and substantially improves the mechanical properties of Si_3N_4 ceramics. Fig. 5 shows the pore size distribution of the porous Si_3N_4 ceramic with 5 wt.% Yb_2O_3 sintered at 1700 and 1800 °C. Very fine pores with average sizes of 0.3 and 0.5 μm were obtained in the samples sintered at 1700 and 1800 °C, respectively.

The XRD patterns of Yb_2O_3-doped Si_3N_4 porous ceramics sintered at 1700 and 1800 °C are shown in Fig. 6. The main phase in the samples was β-Si_3N_4, although some α-Si_3N_4 still remained on certain occasions. The secondary phase was $Yb_4Si_2O_7N_2$ alone,

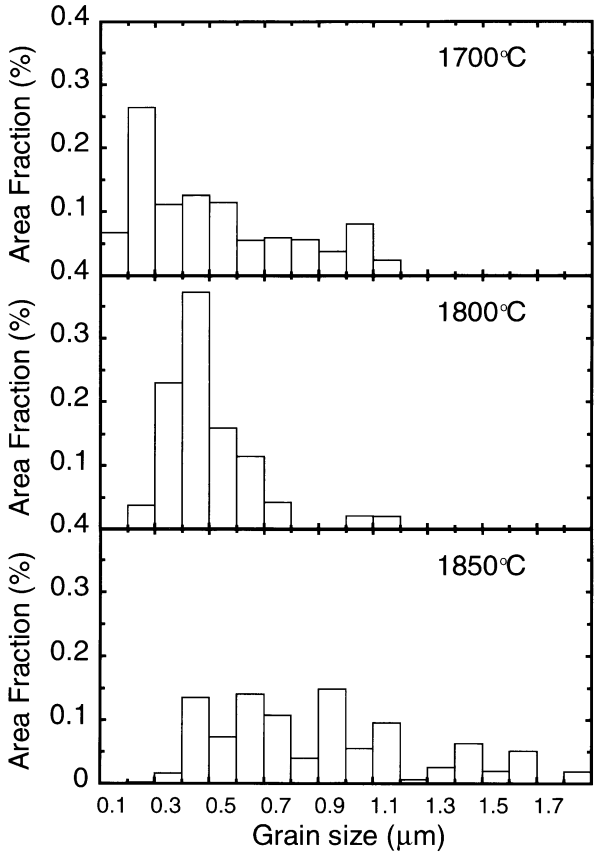

Fig. 4. Grain width distribution of porous Si_3N_4 ceramics with 5 wt.% Yb_2O_3. The specimens were sintered at 1700 °C, 1800 °C and 1850 °C, respectively.

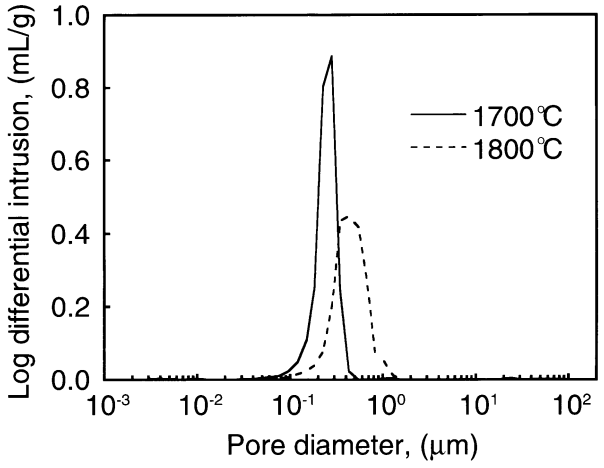

Fig. 5. Pore size distribution of porous Si_3N_4 ceramics with 5 wt.% Yb_2O_3. The specimens were sintered at 1700 °C and 1800 °C, respectively.

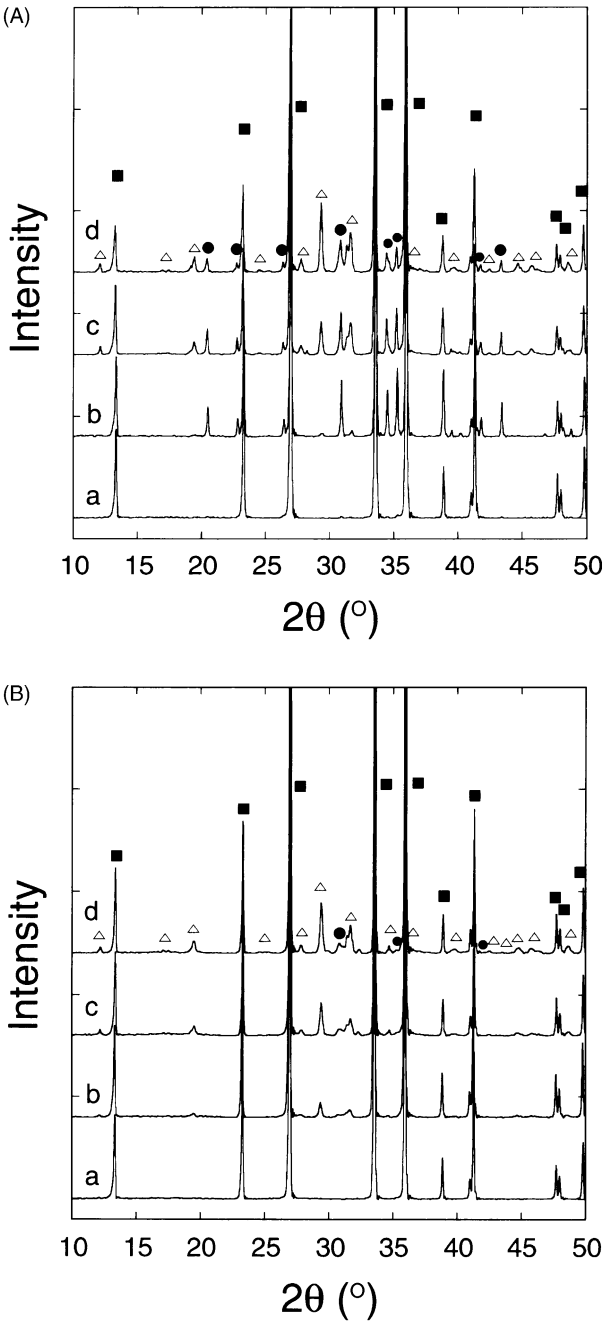

Fig. 6. X-ray diffraction patterns of Si_3N_4 porous ceramic sintered at (A) 1700 °C, (B) 1800 °C with the Yb_2O_3 content of (a) 1.0 wt.%, (b) 2.5 wt.%, (c) 5 wt.%, and (d) 7.5 wt.%. (■) β-Si_3N_4, (●) α-Si_3N_4 and (△) $Yb_4Si_2O_7N_2$.

formed by the reaction between Yb_2O_3 and SiO_2 on the surface of the Si_3N_4 particles, and some Si_3N_4. At a sintering temperature of 1700 °C, the sample with 1 wt.% Yb_2O_3 was composed of β-Si_3N_4, with very small amount of α-Si_3N_4 and secondary phase [Fig. 6(A)(a)], implying an almost complete α-β phase transformation. Increasing the Yb_2O_3 content led to an increase of the secondary phase, as expected, and the α-Si_3N_4 appeared at the same time [Fig. 6(A)(b)–(d)]. The remaining α-Si_3N_4 also was observed by SEM, as shown in Fig. 2, where some small, equiaxed grains are clearly visible. The same tendency also occurred for the samples sintered at 1800 °C, as shown in Fig. 6(B). The difference is that the intensity of the α-Si_3N_4 peak decreased at a high sintering temperature for those samples.

Delayed phase transformation is contradictory to the enhancement of grain growth, because the two processes are closely correlated. Grain growth is accelerated by α–β phase transformation.[19] Phase transformation and grain growth in Si_3N_4 ceramics are enhanced by solution-reprecipitation, which is controlled by either the diffusion of silicon and nitrogen ions through the boundary phase or their reaction (solution-reprecipitation) at the interface between the boundary and the matrix.[20] Thus, phase transformation should be enhanced by Yb_2O_3 addition. Moreover, some authors also report many more large, elongated grains at the outside region of the sample than at the inner region when 4.0 wt.% Yb_2O_3 is used and the sample is prepared by gas-pressure sintering.[21] Yb_2O_3 evaporation in the outer region is more serious, which causes a decrease in Yb_2O_3 content and enhances grain growth.

Three possible reasons explain the incomplete α–β phase transformation with increased Yb_2O_3 addition. First, the viscosity of the glass phase becomes high, because of the lack of Al_2O_3 addition. This increased viscosity makes the phase transformation diffusion-controlled, rather than interfacial-reaction-controlled. Furthermore, diffusion is delayed when the additive content increases. Second, Yb_2O_3 will react with SiO_2 and Si_3N_4 to form $Yb_4Si_2O_7N_2$ crystal:[14]

$$4Yb_2O_3 + SiO_2 + Si_3N_4 = 2Yb_4Si_2O_7N_2$$

The formation of crystallized $Yb_4Si_2O_7N_2$ requires a Yb_2O_3:SiO_2 molar ratio of 4:1, which is ~80:3 by weight. Thus, little of the SiO_2 in the Si_3N_4 powder is consumed, and the remaining Yb_2O_3 and SiO_2 reacts with the Si_3N_4 to form a Si–N–Yb–O glass phase. Therefore, increasing the Yb_2O_3 content resulted in the increasing of $Yb_4Si_2O_7N_2$ content,[14] with a decreasing of the Si–N–Yb–O glass phase. As a result, the phase transformation is somewhat insufficient, because of the decreased glass phase. Third, the solubility of lanthanide ions in the Si_3N_4 is different for α- than for β-crystals;[22] that is, lanthanide ions can dissolve into the α-Si_3N_4 matrix, but not into the β-Si_3N_4. Thus, the solutions of lanthanide ions enhance the Si–N bond and impede the phase transformation of α-Si_3N_4 to β-Si_3N_4. The delayed α–β transformation probably makes a positive contribution to the high-temperature properties of the Si_3N_4 ceramics.

3.3. Mechanical properties

The flexural-strength values of the samples are shown in Fig. 7, as a function of additive content and sintering temperature. The strength increases with additive content and sintering temperature. An increase in density basically contributes to the strength; however, other factors also affect the strength of the samples, as shown below.

Flexural strength, as a function of porosity, is shown in Fig. 8, in which the two solid lines represent the

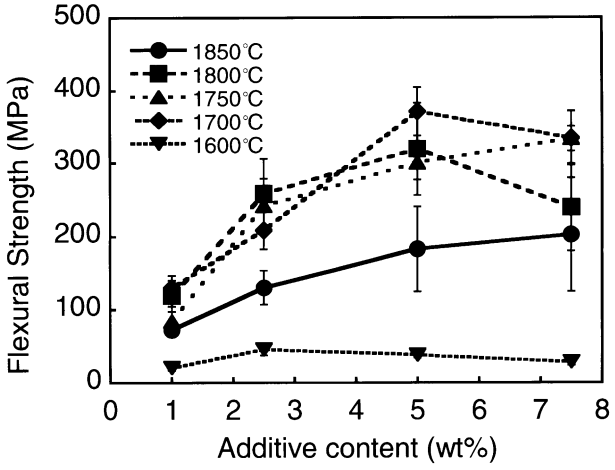

Fig. 7. Flexural strength as a function of Yb_2O_3 content for Si_3N_4 porous ceramic prepared under different sintering conditions.

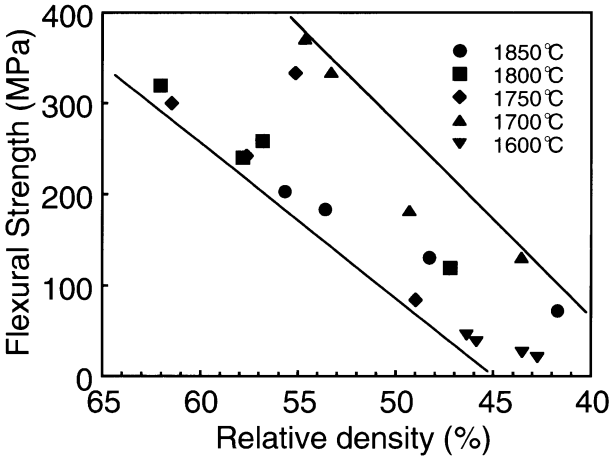

Fig. 8. Relationship between flexural strength and porosity for Si_3N_4 porous ceramic.

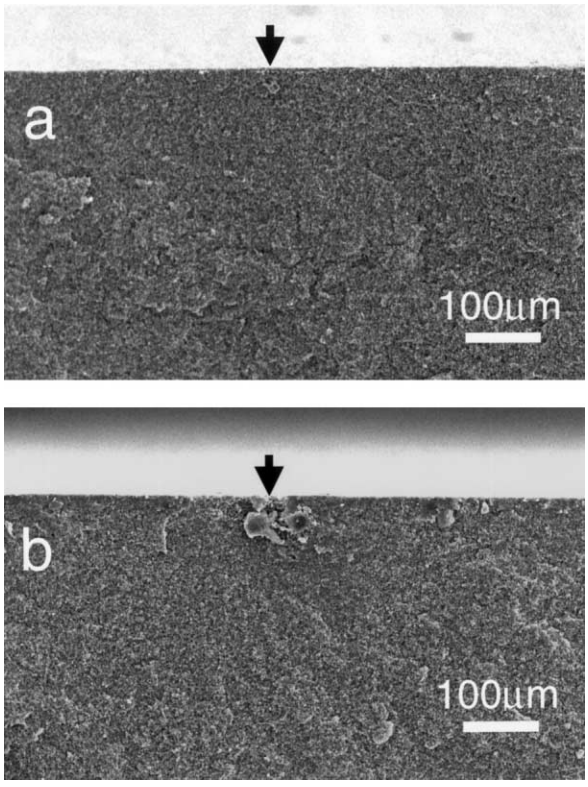

Fig. 9. SEM photographs of fracture surfaces for the samples with 5 wt.% Yb_2O_3: (a) small pores in sample sintered at 1700 °C and (b) large pores in sample sintered at 1800 °C.

region of strength distribution. Clearly, the flexural strength decreases as porosity increases. As shown in Fig. 8, the flexural strength of the samples sintered at a relatively low temperature, 1700 °C, is located near the upper limit, indicating a high strength level. Changing the sintering conditions and additive contents causes different strength values, with the same porosity.

Fibrous β-Si_3N_4 grains are known to enhance the flexural strength of Si_3N_4 porous ceramics,[6] most likely because the fibrous β-Si_3N_4 grains are beneficial for strengthening by grain bridging and pullout. When the present sample was sintered at 1600 °C, at which little phase transformation occurred, the flexural strength was very low. Usually, phase transformation starts in the temperature range 1600–1650 °C, and grain growth starts at the same time. Of course, increasing the sintering temperature would accelerate the development of large, elongated grains. In the present study, high strength was obtained for the samples sintered at 1700 °C, which indicates that fine-sized, fibrous Si_3N_4 grains, rather than coarse grains, favor high strength in porous Si_3N_4 ceramics.

Strength is governed by weakest link statistics, and it is the largest pores with their pronounced internal stress concentration that determines the strength.[23,24] SEM fractography of fracture origins of the samples with 5 wt.% Yb_2O_3 are shown in Fig. 9 for sintering at (a) 1700 °C and (b) 1800 °C. It can be seen that there were no apparent fracture origins for the samples sintered at 1700 °C [Fig. 9(a)], however, fracture origins with size of ~50 μm could be detected for the samples sintered at 1800 °C [Fig. 9(b)], which resulted in the low strength. The defect was formed by the agglomerate of the pore and glass phase during the sintering.

The average width of Si_3N_4 grain, Young's modulus, and calculated strain-to-failure, together with the density and flexural strength, for some selected samples are listed in Table 2. In general, Young's modulus decreases with decreasing density, becoming as low as ~70 GPa for samples with ~50% of theoretical density. The Si_3N_4 with 5 wt.% Yb_2O_3 sintered at 1700 °C (sample 2 in Table 2) has a high strength, up to 370 MPa, and a low Young's modulus, as low as 73 GPa, resulting in a strain-to-failure of 5×10^{-3}.

Usually, dense Si_3N_4 ceramics have a strength of 800–900 MPa and a Young's modulus of 310 GPa, and the strain-to-failure is $\sim2.5\times10^{-3}$ to 3×10^{-3}. Thus, sample 2 in Table 2 has a strain-to-failure twice as high as that of dense Si_3N_4. At the same time, the increase in the average width of grain decreases the strength; as a result, the strain-to-failure decreases correspondingly. Moreover, the strength of the sample with 2.5 wt.% Yb_2O_3 sintered at 1700 °C is lower than that sintered at 1800 °C, because of the low density. However, a high strain-to-failure is obtained at 1700 °C, because of the significant decrease in Young's modulus.

Table 2
Relative density, average width of grain, flexural strength, Young's modulus and strain-to-failure of selected porous Si_3N_4 ceramic

Sample number	Yb_2O_3 content (wt.%)	Sintering conditions	Relative density (TD%)	Average width of grain (μm)	Flexural strength (MPa)	Young's modulus (GPa)	Strain to failure ($\times10^{-3}$)
1	5	1600 °C, 2	45.9		38±3.7		
2	5	1700 °C, 2	56.6	0.26	371±33	73.4	5.06
3	5	1800 °C, 2	62.0	0.37	320±50	102.5	3.12
4	5	1850 °C, 2	53.6	0.47	183±48	70.6	2.59
5	2.5	1700 °C, 2	49.3	0.22	182±25	47.1	3.86
6	2.5	1800 °C, 2	56.8	0.35	259±47	87.5	2.96

4. Conclusions

1. Si_3N_4 ceramics with one type of Yb_2O_3 additive showed low sinterability. In the temperature range 1600–1850 °C, porous Si_3N_4 ceramics, with 40–60% porosity, were obtained.
2. The microstructure of the sample with a high Yb_2O_3 content exhibited many large, elongated β-Si_3N_4 grains. However, phase transformation was impeded because of the formation of crystalline $Yb_4Si_2O_7N_2$ and the dissolution of ytterbium ions. Moreover, a high sintering temperature accelerated the development of coarse, elongated β-Si_3N_4 grains.
3. Excellent mechanical properties were obtained by optimizing the sintering conditions and additive content. For the microstructure with fine, fibrous β-Si_3N_4 grains and fine pore, high flexural strength and strain to fracture were obtained.

Acknowledgements

This work has been supported by AIST, MITI, Japan, as part of the Synergy Ceramics Project. The authors are members of the Joint Research Consortium of Synergy Ceramics.

References

1. Lange, F. F., Tu, W. C. and Evans, A. G., Processing of damage tolerant, oxidation resistant CMC's by a precursor infiltration and pyrolysis method. *Mat. Sci. and Eng*., 1995, **A195**, 145–150.
2. Tu, W. C. and Lange, F. F., Liquid precursor infiltration and pyrolysis of powder compacts, I: kinetic studies and microstructure development. *J. Am. Ceram. Soc*., 1995, **78**(12), 3277–3282.
3. Haslam, J. J., Beroth, K. E. and Lange, F. F., Processing and properties of an all-oxide composite with a porous matrix. *J. Eur. Ceram. Soc*., 2000, **20**, 607–618.
4. Kanaka, B. and Schneider, H., Aluminosilicate fiber/mullite matrix composites with favorable high-temperature properties. *J. Eur. Ceram. Soc*., 2000, **20**, 619–623.
5. Shigegaki, Y., Brito, M. E., Hirao, K., Toriyama, M. and Kanzaki, S., Strain tolerant porous silicon nitride. *J. Am. Ceram. Soc*., 1997, **80**(2), 495–498.
6. Kawai, C. and Yamakawa, A., Effect of porosity and microstructure on the strength of Si_3N_4: designed microstructure for high strength, high thermal shock resistance and facile machining. *J. Am. Ceram. Soc*., 1997, **80**(10), 2705–2708.
7. Inagaki, Y., Ohji, T., Kanzaki, S. and Shigegaki, Y., Fracture energy of an aligned porous silicon nitride. *J. Am. Ceram. Soc*., 2000, **83**(7), 1807–1809.
8. Yang, J. F., Zhang, G. J. and Ohji, T., Fabrication of low-shrinkage, porous silicon nitride ceramics by addition of a small amount of carbon. *J. Am. Ceram. Soc*., 2001, **84**(7), 1639–1641.
9. Yang, J. F., Zhang, G. J. and Ohji, T., Porosity and microstructure control of porous ceramics by partial hot-pressing. *J. Mater. Res*., 2001, **16**(7), 1916–1918.
10. Nanjangud, S. C., Brezny, R. and Green, D. J., Strength and Young's Modulus Behavior of a Partially Sintered Porous Alumina. *J. Am. Ceram. Soc*., 1995, **78**(1), 266–268.
11. Lam, D. C. C., Lange, F. F. and Evans, A. G., Mechanical properties of partially dense alumina from powder compacts. *J. Am. Ceram. Soc*., 1994, **77**(8), 2113–2117.
12. Wang, C. M., Pan, X., Hoffmann, M. J., Cannon, R. M. and Rühle, M., Grain boundary films in rare-earth-glass-based silicon nitride. *J. Am. Ceram. Soc*., 1996, **79**(3), 788–792.
13. Nishimura, T. and Mitomo, M., Phase relationship in the system Si_3N_4-SiO_2-Yb_2O_3. *J. Mater. Res*., 1995, **10**(2), 240–242.
14. Park, H. J., Kim, H. E. and Niihara, K., Microstructural evaluation and mechanical properties of Si_3N_4 with Yb_2O_3 as a sintering additive. *J. Am. Ceram. Soc*., 1997, **80**(3), 750–756.
15. Suttor, D. S. and Fischman, G. S., Densification and sintering kinetics in sintered silicon nitride. *J. Am. Ceram. Soc*., 1992, **75**(5), 1063–1067.
16. Yang, J. F., Ohji, T. and Niihara, K., The influence of Y_2O_3-Al_2O_3 content on sintering process and microstructure of silicon nitride ceramics. *J. Am. Ceram. Soc*., 2000, **83**(8), 2094–2096.
17. Raj, R. and Hoffmann, M. J., Thermodynamic analysis of grain aspect ratio in fibrous microstructure of silicon nitride. *J. Am. Ceram. Soc*., 1997, **80**(12), 3250–3252.
18. Park, D. S., Lee, S. Y., Kim, H. D., Yoo, B. J. and Kim, B. A., Extra-large grains in the silicon nitride ceramics doped with yttria and hafnia. *J. Am. Ceram. Soc*., 1998, **81**(7), 1876–1880.
19. Emoto, H., Hirotsuru, H. and Mitomo, M., Influence of phase transformation on grain growth behavior of silicon nitride ceramics. *Key Engineering Materials*, 1999, **159–160**, 215–220.
20. Lifzhitz, I. M. and Slyozov, V. V., The kinetics of precipitation from supersaturated solid solution. *J. Phys. Chem. Solid*, 1961, **19**(1/2), 35–50.
21. Lee, K. M., Lee, W. H., Koh, Y. H., Choi, J. J., Kim, H. E. and Baek, S. S., Microstructural evaluation and mechanical properties of gas-pressure-sintered Si_3N_4 with Yb_2O_3 as a sintering aids. *J. Mater. Res*., 1999, **14**(5), 1904–1909.
22. Nakayasu, T., Yamada, T., Tanaka, I., Adachi, H. and Goto, S., Local chemical bonding around rare-earth ions in α- and β-Si_3N_4. *J. Am. Ceram. Soc*., 1997, **80**(10), 2525–2532.
23. Rice, R. W., Pores as fracture origins in ceramics. *J. Mater. Sci*., 1984, **19**, 895–914.
24. Ostrowski, T., Ziegler, A., Bordia, R. K. and Rödel, J., Evaluation of young's modulus, strength, and microstructure during liquid-phase sintering. *J. Am. Ceram. Soc*., 1998, **81**(7), 1852–1860.